

Supplement of Atmos. Chem. Phys., 18, 621–634, 2018
<https://doi.org/10.5194/acp-18-621-2018-supplement>
© Author(s) 2018. This work is distributed under
the Creative Commons Attribution 4.0 License.



Supplement of

Response to marine cloud brightening in a multi-model ensemble

Camilla W. Stjern et al.

Correspondence to: Camilla W. Stjern (camilla.stjern@cicero.oslo.no)

The copyright of individual parts of the supplement might differ from the CC BY 4.0 License.

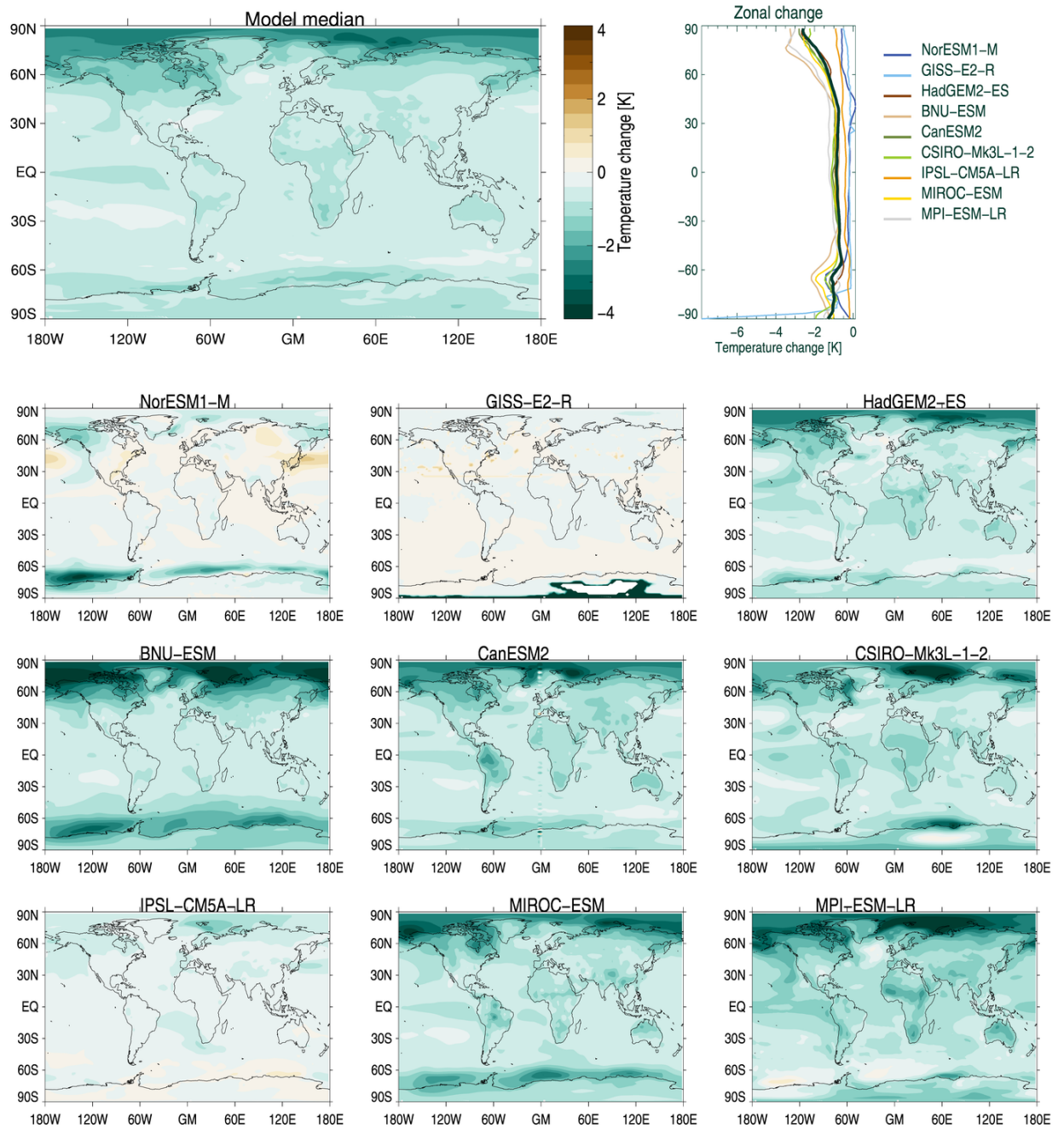


Figure S1: Near-surface temperature changes (K) for all models, as well as for the model median.

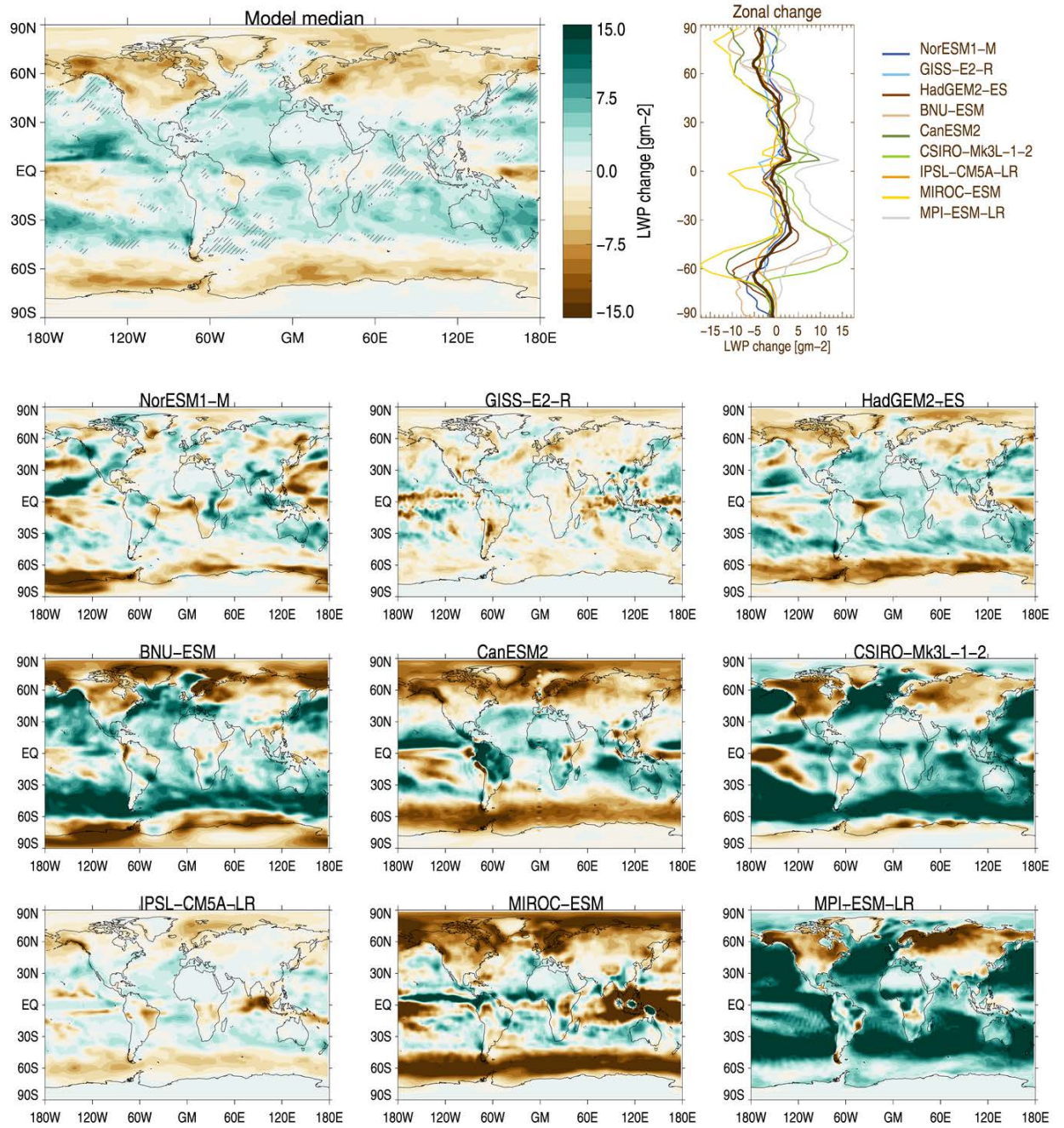


Figure S2: LWP changes (%) for all models, as well as for the model median.

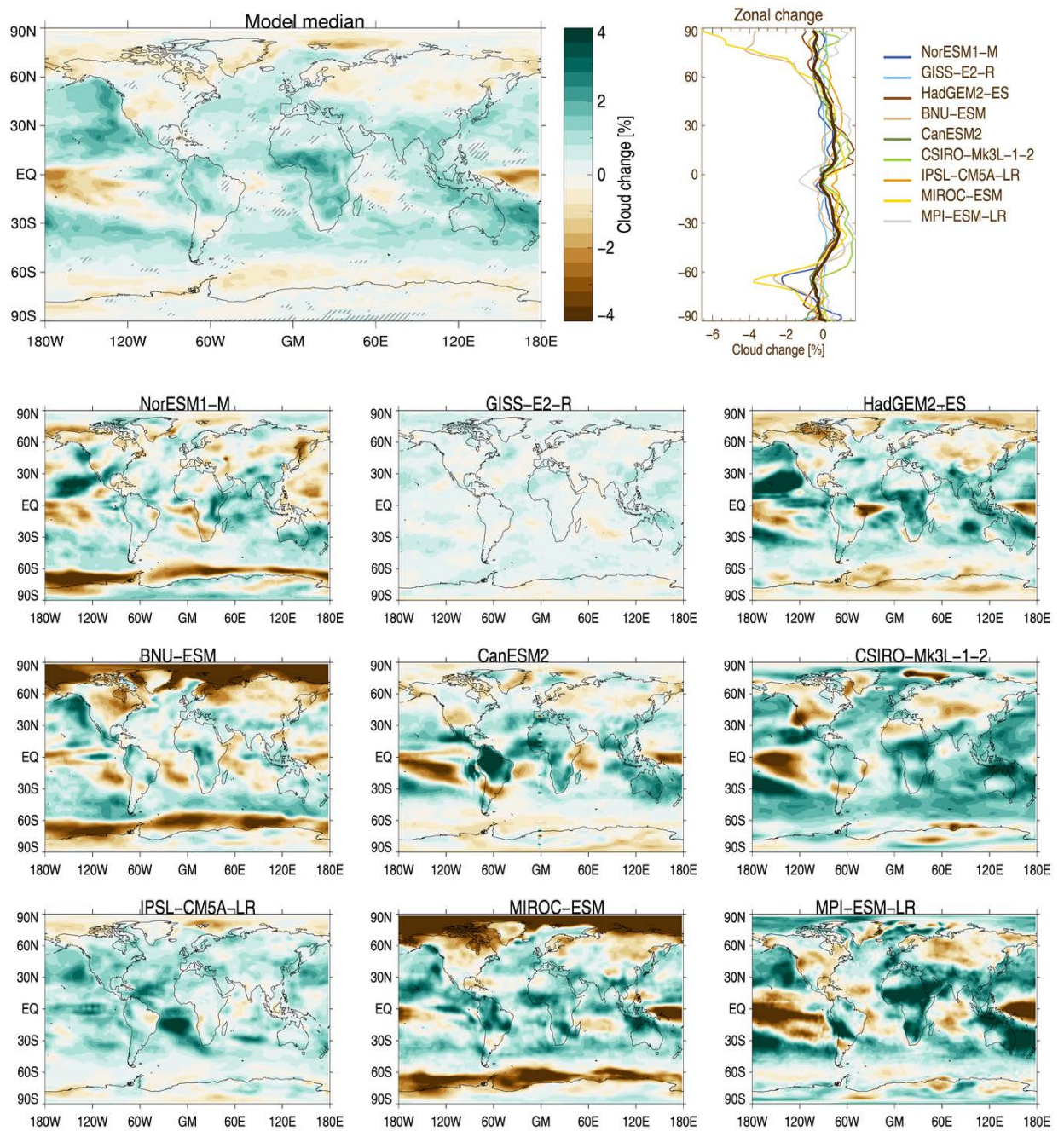


Figure S3: Absolute total cloud changes (%) for all models, as well as for the model median.

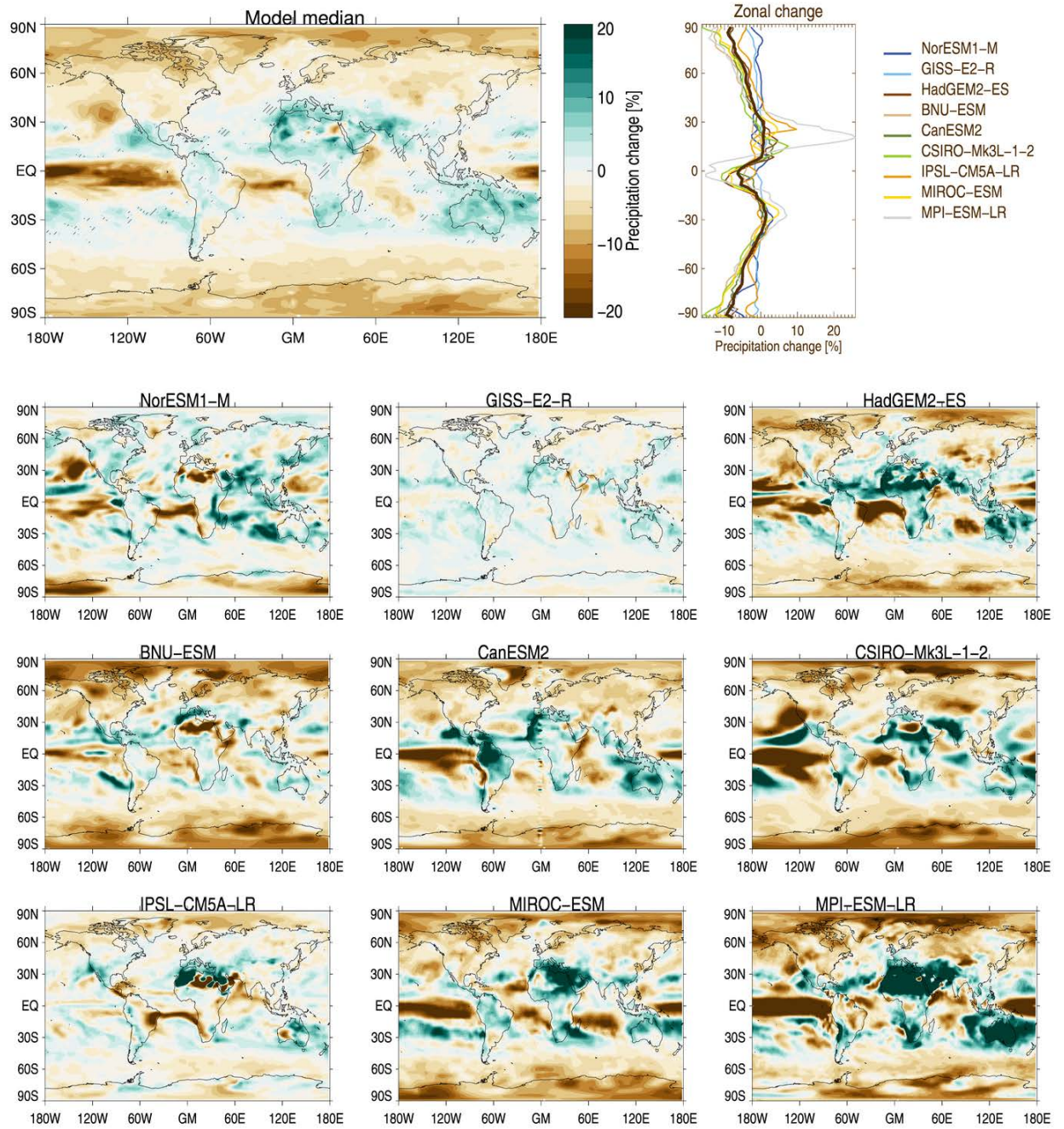


Figure S4: Precipitation changes (%) for all models, as well as for the model median.

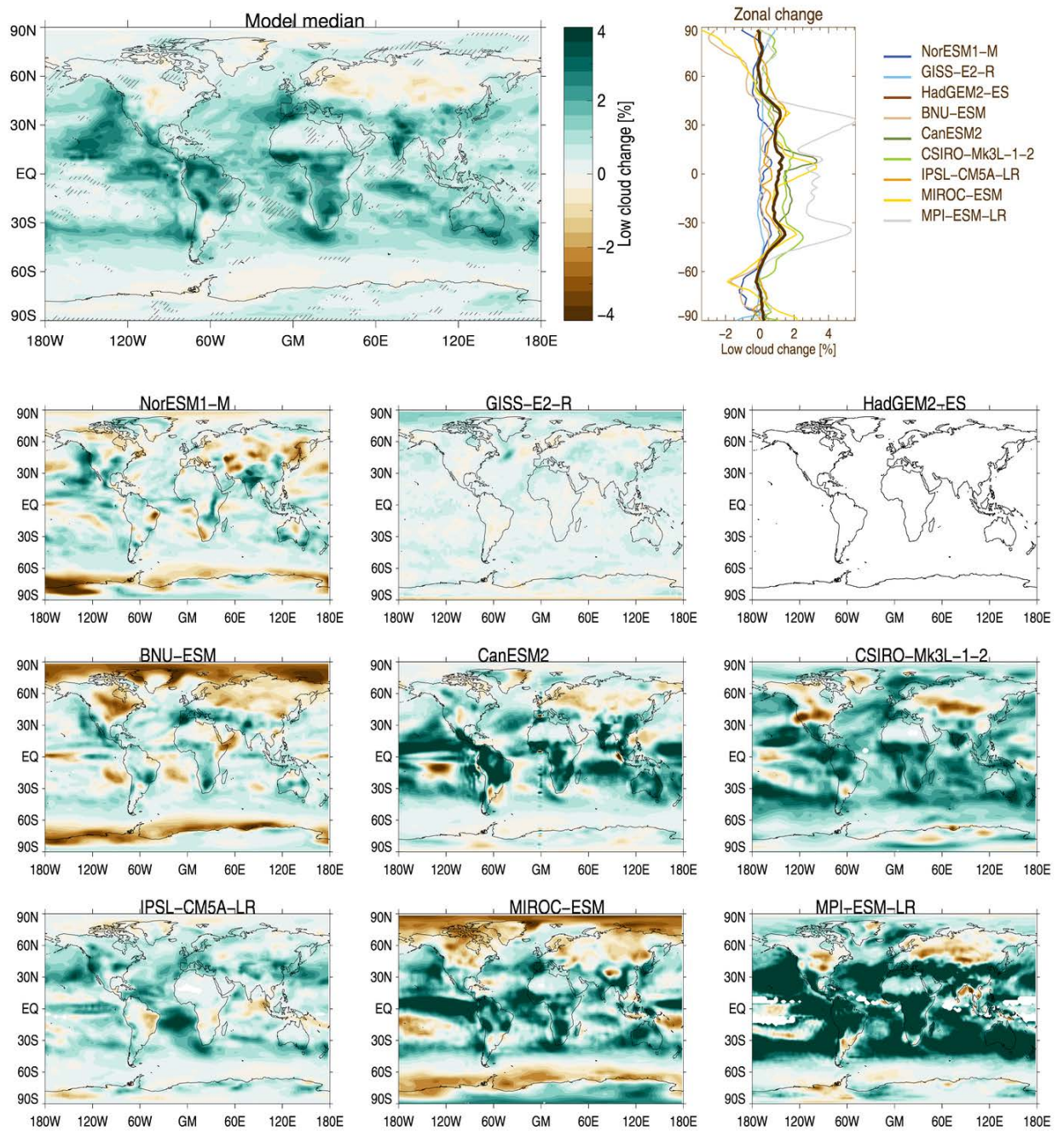


Figure S5: Absolute low cloud changes (%) for all models, as well as for the model median. Data were not available for HadGEM2.

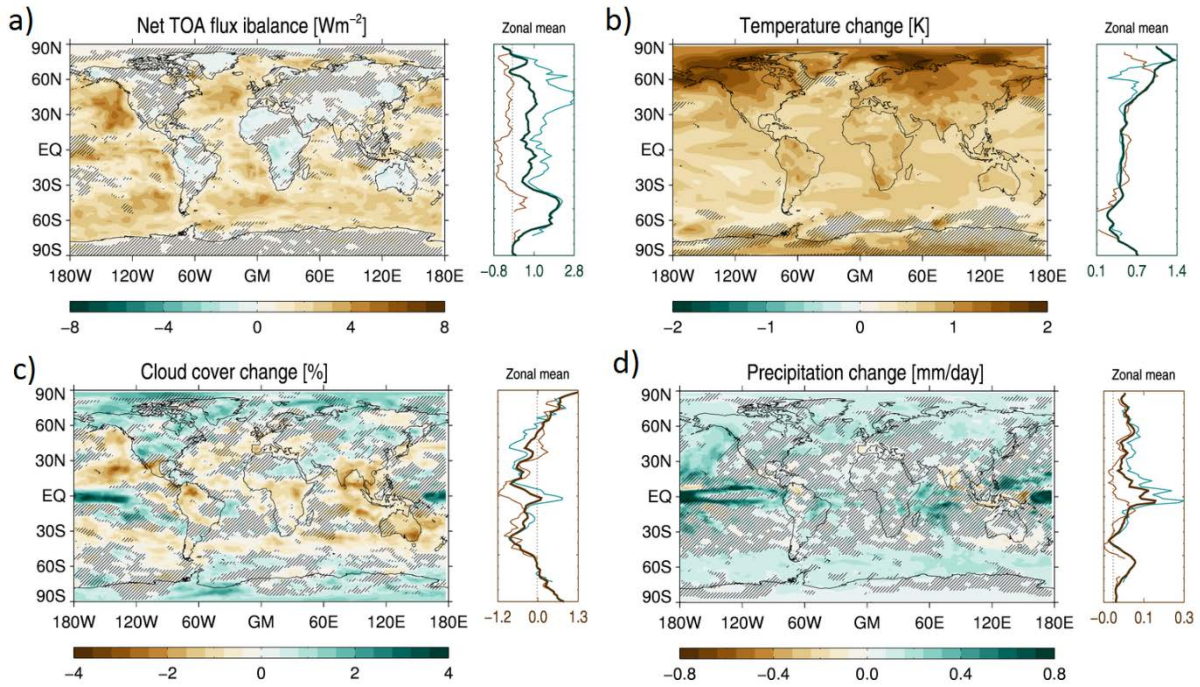


Figure S5: Termination effect. First, the mean change for the G4cdc years 2050-2069 (the last 20 years of the geoengineering period) is subtracted from the termination period 2070-2089, and the difference for the corresponding years of the RCP4.5 simulations are then subtracted from this number. This gives us an estimate of how much stronger the climate change from abrupt suspension of geoengineering is than the change for the corresponding period for RCP4.5. Panels show ensemble median (taken in each grid cell) differences in a) TOA net radiative flux imbalance (Wm^{-2}), b) near-surface air temperature change (K), c) total cloud cover (%), and d) precipitation (%). Hatched areas are grid cells where less than 75 % of the models agreed on the sign of the change. Zonal averages are given to the right of each panel, where brown and blue lines indicate land-only and ocean-only averages.

	Correlation between surf. temp. change and TOA rad. flux imbalance	Correlation between surf. temp. change and baseline low cloud fraction	Correlation between surf. temp. change and baseline LWP for oceans
	Global mean correlation	Spatial correlation	Spatial correlation
BNU-ESM	-0.60	-0.52	-0.47
CanESM2	-0.83	-0.18	+0.40
CSIRO-Mk3L-1-2	-0.92	-0.22	+0.41
GISS-E2-R	-0.26*	+0.05	+0.01
HadGEM2-ES	-0.69	-0.21	+0.51
IPSL-CM5A-LR	-0.35*	+0.06	+0.21
MIROC-ESM	-0.56	-0.43	+0.47
MPI-ESM-LR	-0.85	-0.14	+0.19
NorESM1-M	-0.29*	-0.39	-0.30
Median	-0.55	-0.30	+0.42

Table S1: For the global mean correlations (leftmost column), globally and annually averaged temperature changes over the years 2020-2069 are correlated against corresponding changes in TOA radiative flux imbalance. For the spatial correlations (two rightmost columns), global matrices of annual mean changes (average of years 2020-2069) are correlated against baseline (20 first year of RCP4.5) values. All correlations except those marked by an asterisk are statistically significant on the 95% level. The lowest row shows correlation between model-median quantities (not the median of the individual model values above).

	Arctic amplification for RCP4.5	Arctic amplification for G4cdnc
BNU-ESM	6.6	1.7
CanESM2	3.6	2.0
CSIRO-Mk3L-1-2	3.8	0.6
GISS-E2-R	2.1	---
HadGEM2-ES	3.8	0.9
IPSL-CM5A-LR	1.9	2.0
MIROC-ESM	1.1	---
MPI-ESM-LR	---	---
NorESM1-M	2.1	-0.5
Median	3.6	1.7

Table S2: Arctic amplification for the termination period, estimated as the mean temperature change (average of 2070-2089 minus average of 2050-2069) for the Arctic (defined as all area above 60° N) divided by the globally averaged temperature change. Leftmost column shows numbers for RCP4.5 while rightmost column shows changes for G4cdnc. Models that did not simulate the termination period is marked with '---'.